Marine Mammal Science

NOTE OPEN ACCESS

Preserving an Imperiled Porpoise Through Pixels: Digitization of a Vaquita (*Phocoena sinus*) Skeleton, the World's Most Endangered Marine Mammal

Jamie L. Knaub[1,2] | Brittany A. Dolan[3,4] | Philip Unitt[5] | Robert L. Brownell Jr.[6] | Tricia L. Meredith[2] | Marianne E. Porter[1]

[1]Department of Biological Sciences, Florida Atlantic University, Boca Raton, Florida, USA | [2]FAU Lab Schools, Florida Atlantic University, Boca Raton, Florida, USA | [3]Animal Health and Rescue, SeaWorld California, San Diego, California, USA | [4]The Marine Mammal Center, Sausalito, California, USA | [5]Department of Birds and Mammals, San Diego Natural History Museum, San Diego, California, USA | [6]NOAA Fisheries, Southwest Fisheries Science Center, La Jolla, California, USA

Correspondence: Jamie L. Knaub (jknaub2020@fau.edu) | Robert L. Brownell Jr (robert.brownell@noaa.gov)

Received: 31 October 2025 | **Revised:** 21 January 2026 | **Accepted:** 16 March 2026

Keywords: 3D imaging | cetacean | computed tomography (CT) | educational resources | MorphoSource | natural history collections

The porpoise genus *Phocoena* (family Phocoenidae) comprises four species that are found mainly in cold coastal waters. The harbor porpoise (*P. phocoena*) is found along the western and eastern coasts of the North Pacific and North Atlantic, whereas the Burmeister's porpoise (*P. spinipinnis*) occurs along much of the western coast of South America and the southern half of the eastern coast. The spectacled porpoise (*P. dioptrica*) is found in the southern waters off Argentina and subantarctic islands including the Falklands/Malvinas, South Georgia, Kerguelen, Heard, Macquarie, and Auckland. The vaquita (*P. sinus*) is the smallest extant cetacean and occupies an extremely small range, exclusively the relatively shallow waters of the northern Gulf of California, Mexico (Jefferson et al. 2015). Across the four *Phocoena* species, early descriptions of porpoise skeletal anatomy were limited to *P. phocoena* (Tyson 1680) and *P. spinipinnis* (Burmeister 1865), while skeletal descriptions for *P. dioptrica* (Graïc et al. 2025; Lahille 1912; Perrin et al. 2000) and *P. sinus* (Brownell 1983; Magatagan et al. 1984; Noble and Fraser 1971; Torre-Cosio 1995) have been published more recently.

The northern Gulf of California has biologically rich waters from strong tidal mixing and upwelling, attracting intensive fishing for sharks, rays, mackerels, corvinas, and shrimps (Vidal et al. 2024). While the vaquita's pre-exploitation population is thought to have been naturally small, less than 5000 individuals, the first robust survey conducted in 1997 indicated that the population was already fewer than 600 individuals (Jaramillo-Legorreta et al. 1999; Morin et al. 2021; Robinson et al. 2022; Rojas-Bracho and Taylor 1999; Vidal et al. 2024). A later assessment in 2015 estimated the population decreased to 59 individuals, a 92% decline, and in 2018, it was estimated that fewer than 20 vaquita remained (Jaramillo-Legorreta et al. 1999, 2019; Taylor et al. 2017). As a result, surveys have become more frequent and intensive, including line transects, acoustic monitoring, and the establishment of a photo-identification database (Gerrodette et al. 1995, 2011; Jaramillo-Legorreta et al. 1999, 2017, 2019, 2023; Jefferson et al. 2009; Rojas-Bracho, Booth, et al. 2019a; Rojas-Bracho, Brusca, et al. 2019b; Rojas-Bracho et al. 2022; Rojas-Bracho, Gulland, et al. 2019c; Taylor et al. 2017, 2019; Taylor and Gerrodette 1993; Thomas et al. 2017). In 2019, surveys started to use a technique called "expert elicitation" where expert judgments are combined with available data to create an informed assessment (Rojas-Bracho, Booth, et al. 2019a). These more recent annual surveys report the number of distinct individual vaquitas observed within the study area and represent a minimum estimate for the population, as individuals may occur outside this area. The 2023 survey reported a 67% probability that 8–12 different vaquitas were observed, and the 2024 survey reported a 75% probability that a minimum of 6–8 unique individuals remained (Jaramillo-Legorreta et al. 2023; Cardenas-Hinojosa et al. 2024). However, in 2025, surveys yielded a 75% probability that the population was between 7 and 10 (Cárdenas-Hinojosa et al. 2025).

The vaquita's rapid decline is attributed to the incidental take of individuals via fishing gear, particularly in gillnets targeting the endemic totoaba (*Totoaba macdonaldi*) (Vidal et al. 2024). The totoaba is a teleost fish, the largest species of the family Sciaenidae; it reaches up to two meters in length, while the maximum length recorded for the vaquita is 1.5 m (Cisneros-Mata 2020; Vidal 1995; Vidal et al. 2024). The swim bladder of the totoaba has significant value on the Mexican black market and is worth more when exported to the United States and Asia, particularly to Chinese markets (Ben-Hasan et al. 2021; Valenzuela-Quiñonez et al. 2015). Despite the Mexican government banning the totoaba fishery in 1975, fishing continues and the illegal trading and export of swim bladders is run by deeply rooted organized crime networks (Aceves-Bueno et al. 2023; Ben-Hasan et al. 2021; Cisneros-Mata 2020; Cisneros-Mata et al. 1995; D'Agrosa et al. 1995, 2000; Lagomarsino 1991; Román-Rodríguez 1990; Vidal 1995). In the last decade, extreme efforts aimed at reducing bycatch and protecting the remaining vaquitas have included involvement from the conservation group Sea Shepherd and the Mexican Navy to remove gillnets, the emergency international and multi-institutional field effort of VaquitaCPR, and the establishment of the Zero Tolerance Area for gillnets by the Mexican Navy (Rojas-Bracho, Gulland, et al. 2019). After two unsuccessful attempts at captive care through VaquitaCPR, efforts to take the remaining vaquita into temporary holding for preservation ceased (Rojas-Bracho, Gulland, et al. 2019). As a result, preventing the imminent extinction of the vaquita will likely take immediate and coordinated efforts from Mexico, China, and the United States.

Despite continued advocacy and conservation efforts, the future of the vaquita is uncertain, and preservation of its natural history is a crucial component of ongoing and future study. Here, we describe the development of an open-access dataset of 2D images, high-resolution 3D micro-computed tomography (micro-CT) scans, and 3D meshes of a vaquita skeleton for use by scientists, educators, students, and the public. We have made all products of this digitization project (scans, photos, and meshes) freely available via MorphoSource, a digital repository of media representing physical objects important to the world's natural history, cultural heritage, and scientific collections (Boyer et al. 2016). We aim to increase awareness of the vaquita's status, encourage use of open-access resources, and contribute to the existing datasets associated with this critically endangered marine mammal.

The advancement of imaging technologies over the past decade has prompted large-scale digitization initiatives that are transforming biological science through the creation of open-access, high-fidelity 3D representations of natural history specimens (Blackburn et al. 2024; Weisbecker et al. 2025). Recently, the openVertebrate (oVert) Thematic Collections Network, funded by the United States National Science Foundation (NSF), spearheaded a community effort resulting in the digitization of over 13,000 vertebrate specimens from US-based natural history collections. The digitized specimens represent more than 80% of extant vertebrate genera, including a subset of families that were contrasted to capture soft-tissue anatomy (Blackburn et al. 2024; Gray et al. 2025). Similarly, Ozboneviz is a FAIR (findable, accessible, interoperable, reusable) open-access collection of 3D imagery of Australian vertebrates (Weisbecker et al. 2025). Projects like oVert and Ozboneviz generate resources and other widely available digital datasets of museum collections that exponentially expand global access to specimens that were previously only available through photographs or direct, often restricted, physical examination (Blackburn et al. 2024; Weisbecker et al. 2025). As part of the broader movement of specimen digitization, the vaquita dataset presented here not only contributes to the growing body of digital vertebrate resources but also highlights the potential use of open-access collections to inform, educate, and inspire global conservation efforts.

The specimen digitized for this project was a female vaquita (139 cm total length) collected by Robert L. Brownell Jr. (RLB) on April 24, 1966, approximately 24 km north of San Felipe, Baja California, Mexico (31.21° N, 114.88° W). In 1966, RLB deposited the specimen (formally known as RLB 221), along with partial skeletons of two other individuals, to the San Diego Natural History Museum (SDNHM), where it was entered under accession number 194 and cataloged as SDNHM 20688 (Figure 1). The specimen was first referenced in primary literature in 1973, in a comprehensive morphological study examining the tympano-periotic bones of odontocetes (Kasuya 1973). In 1982, a list of external measurements of SDNHM 20688 was published, and the specimen was referenced the following year in a more thorough assessment of the vaquita (Brownell 1982, 1983). In 1984, Magatagan et al. referenced SDNHM 20688 but listed it as LACM 20688 (Natural History Museum of Los Angeles County), and it was not one of the three vaquita used for postcranial skeletal assessment (Magatagan et al. 1984). However, SDNHM 20688 was one of several vaquita specimens used to define the distribution of *P. sinus* (Brownell 1986). This skeleton was also later examined and used in a comprehensive study investigating cetacean evolutionary relationships and phylogeny (Messenger and McGuire 1998).

The SDNHM loaned the vaquita specimen to SeaWorld California (SWC; San Diego, California) in March of 2024 for a total of 365 days. The skeleton was initially imaged via medical computed tomography scans by the San Diego Zoo Wildlife Alliance. In the subsequent August, the forelimbs were sent to the Museum of Osteology (Oklahoma City, Oklahoma) for removal of the remaining desiccated soft tissues by dermestid beetle colonies. This process revealed the underlying bones with largely intact cartilaginous connections. The right forelimb (Cooper et al. 2007) includes the humerus, radius, ulna, carpals, metacarpals, and phalanges (Video S1). Portions of the left forelimb (humerus, radius, and ulna as one unit, and the most distal phalanges of four digits) remained articulated. The entire skeleton was then transported to Florida Atlantic University (FAU) in Boca Raton, Florida. Upon arrival at FAU, the skeleton was laid out, inventoried, and examined prior to digitization via photography and micro-CT.

The skeleton's digitization through photography and micro-CT scanning proceeded as follows. Initial photographs were taken by Dallas Clites in July 1968 with a 4×5 Calumet View camera and a Schneider 150 mm f/5.6 Symmar-S lens with a Synchro-Compur shutter and 4×5 Kodak Plus-X film. In 2024, the skeleton was imaged via medical CT scans with a NeuroLogica (Samsung subsidiary, Danvers, MA, USA) BodyTom Elite (32-slice, 1.25 mm detector) by the San Diego Zoo Wildlife Alliance.

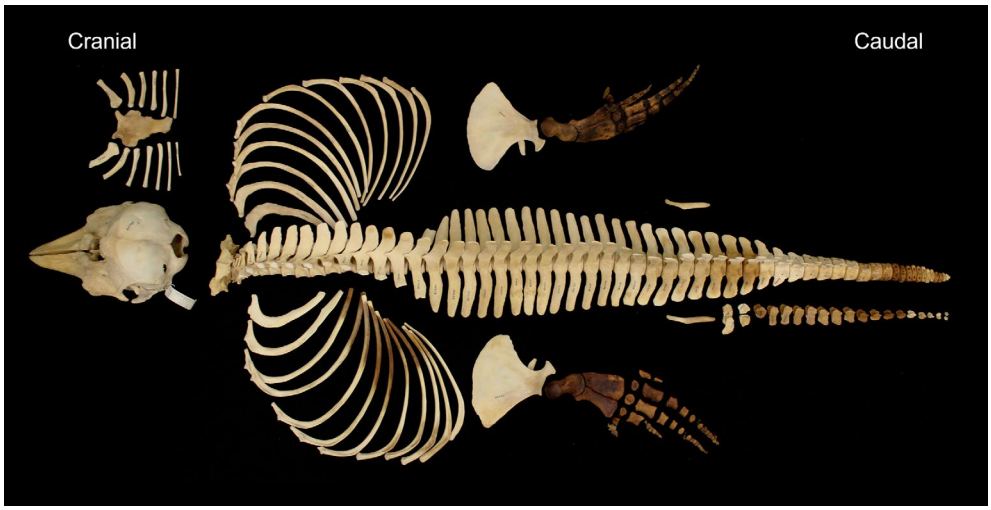

FIGURE 1 | Vaquita (*Phocoena sinus*) skeleton SDNHM 20688 (formally known as RLB 221). The specimen was an adult female (139 cm total length) collected by RLB on April 24, 1966, about 24 km north of San Felipe, Baja California, Mexico. Pictured here is a dorsal view of the skeleton and an internal view of the forelimbs captured by Jamie Knaub in 2024. The sternum and sternal ribs were placed by the skull for ease of viewing. The mandibles, teeth, ear bones, zygomatic arches, and hyoids are not pictured.

Later that same year, SDNHM 20688 was transported to FAU where it was photographed (in groups when appropriate; Table 1) with a scale and static lighting by means of a Canon EOS 50D DSLR camera (Figure 2a–c). For micro-CT scanning, when multiple bones were scanned together, bones were packaged in a plastic canister with polyurethane foam or synthetic sponges to separate the bones from the walls of the canister and other bones. We scanned bones with a Bruker SkyScan 1173 micro-CT system (Kontich, Belgium) at FAU Lab Schools Marcus Research and Innovation Center, Berlin Family Bioimaging Lab (RRID:SCR_023805), with a voxel size ranging from 6.8 to 34.4 μm. We scanned larger bones (skull, mandibles, right forelimb, and true ribs 3–12), which exceeded the chamber size of the Bruker, by using a Waygate Technologies Phoenix v|tome|x m 240 system (Baker Hughes Digital Solutions GmbH, Hürth, Germany) at the University of Florida's Nanoscale Research Facility (RRID:SCR_025135) with a voxel size of 124.9 μm. We reconstructed the scans with NRecon (Bruker) and Phoenix datos|x (Waygate) software and exported derived image stacks for volume rendering and mesh creation (Figure 2d–f). Metadata, including acquisition settings (filter, x-ray voltage and current, exposure time, etc.,) and reconstruction parameters (beam hardening correction, ring artifact correction, etc.,), for all scans are freely available as text files through MorphoSource (see "Description Attachment File" under the Imaging Details section for each medium).

To create mesh files, we imported reconstructed image stacks with respective spacing information (voxel size in mm) via SlicerMorph, an open extension of 3D Slicer software (Rolfe et al. 2021). Using the *Segment Editor* module, we created a segmentation (a digital model) by thresholding (selecting a range of grayscale values from the histogram to separate the area of interest) to isolate each bone (Figure 3a–c). When necessary, tools such as *Paint*, *Erase*, and *Smoothing* were used to optimize segmentations for 3D viewing and printing (Figure 3d–f). The segmentations were then exported as ".stl" files, which are available alongside the photographs and scans of the bones.

The entire skeleton of SDNHM 20688 (Table 1) has a tan coloration, with some bones appearing more yellow or brown, from residual oil. The skull of this specimen was previously described with a condylobasal length of 232 mm and mandibular total length of 171 mm (Figure 4) (Brownell 1983). Additional notable skull measurements include: rostrum length 119 mm, palate length (tip of rostrum to median spine of palate) 116 mm, and brain case width (across the parietals) 113 mm. The skull width with intact zygomatic arches was 140 mm. In its present state, the zygomatic arch bones are preserved but separated from the skull, with the left partially intact and the right preserved in four pieces. The pterygoids are roughly triangular as in the paratype (USNM 303308). The left periotic and malleus are present and unfused. The right periotic and both bullae are missing to date, but photographs are featured in figure 2 of Brownell 1983 and available on MorphoSource (Brownell 1983). The teeth were extracted from the maxilla and mandibles and appear unprocessed (some sand and residual soft tissue present). The number of teeth collected for this specimen (20 left maxilla, 18 right maxilla, 17 left mandible, 18 right mandible) falls within the ranges reported for other vaquita specimens: 16–22 for maxilla rows and 17–20 for mandibular rows (Brownell et al. 1987; Noble and Fraser 1971; Torre-Cosio 1995). The left maxilla has 21 alveoli (tooth sockets), the right maxilla has 20, and there are 20 alveoli in both the left and right mandibles. The length of the left maxilla tooth row is 86 mm.

The hyoid apparatus consists of five bones. The largest is the basihyal, which articulates posterolaterally with the thyrohyal bones. In SDNHM 20688, the basihyal is completely fused to both thyrohyals, forming a "boomerang-shaped" bone (Torre-Cosio 1995). Two ceratohyals are present and ossified, articulating with the stylohyals anterodorsally to the basihyal. The ceratohyals are cartilaginous in most cetaceans and immature vaquita specimens but are ossified in mature vaquitas and harbor porpoises (*P. phocoena*) (Cozzi et al. 2016; Howes 1880; Huggenberger et al. 2008; Reidenberg and Laitman 1994; Torre-Cosio 1995).

TABLE 1 | Comprehensive list of vaquita bones digitized via photographs and micro-CT scans.

Bone	Side/#	Photography notes	Scanning notes
Skull		Photographed separately	Scanned with mandibles*
Mandible	L & R	Photographed separately	Scanned with skull*
Upper Teeth	L 1–20 R 1–18	Stored on tape, photographed together Stored on tape, photographed together	Scanned together Scanned together
Lower Teeth	L 1–16	Stored on notecard, photographed together	Scanned together
	R 1–18	Stored on notecard, photographed together	Scanned together
Zygomatic	L	Photographed separately	Scanned separately
	R	In pieces, photographed together	Scanned together
Ear	L	Periotic & malleus, photographed together	Scanned together
Hyoid Stylohyal Ceratohyal	L & R L & R	Hyoid (fused basihyal & thryohyals), stylohyals, and ceratohyals photographed together	Hyoid, stylohyals, and ceratohyals scanned together
Cervical Vertebrae	1–7	1–3 fused, photographed together (1–7)	Scanned together (1–7)
Thoracic Vertebrae	1–12	Photographed together (1–12)	Scanned in pairs (1–2, 3–4, 5–6, 7–8, 9–10, and 11–12)
Lumbar Vertebrae	1–14	Photographed together (1–14)	Scanned in pairs (1–2, 3–4, 5–6, 7–8, 9–10, 11–12, and 13–14)
Caudal Vertebrae	1–29	Photographed in groups (1–16 and 17–31)	Scanned in pairs (1–2, 3–6, 7–8, 9, 10–14, 15–19, 20–29)
Sternum		Photographed separately	Scanned separately
Sternal Ribs	L 1–7 R 1–6	Photographed in groups (L1–7 and R1–6)	Scanned in groups (L1–4, L5–7, R1–6)
True Ribs	L 1–12 R 1–12	Photographed in groups (L1–12 and R1–12)	Scanned in groups (L1&2, L3–12*, R1&2, R3–12*)
Chevrons	1–19	1, 2, 19 unfused, photographed together (1–19)	Scanned together (1–19)
Pelvic	L & R	Photographed separately	Scanned together
Scapula	L & R	Photographed separately	Scanned together
Forelimb	L	Soft tissue preserved humerus, radius, and ulna together, some smaller phalanges preserved via soft tissue, all photographed together	Scanned in two groups (humerus, radius and ulna) and (carpals, metacarpals and phalanges)
	R	Soft tissue preserved all bones in articulated state, photographed together	Scanned together*

Note: All bones were scanned with a Bruker SkyScan except the skull, mandibles, right forelimb, and true ribs (L & R#3–12) which were scanned with a Waygate Technologies Phoenix (noted with *).

The vertebral formula for the specimen is C7 + T12 + L14 + Ca29 for a total of 62 vertebrae whereas the total vertebral count for *P. phocoena* is reported to range from 62 to 67 (Slijper 1936; Smith et al. 1976). Vertebral regions were defined as follows: cervical—anterioposteriorly compressed vertebrae with a well-defined neural canal; thoracic—vertebrae that articulate with ribs on both left and right transverse processes (i.e., the last thoracic vertebra articulates with a pair of ribs; a single ligamentous or "floating" rib attachment denotes the first lumbar); lumbar—vertebrae with no articulation to a pair of ribs or chevron bones; caudal—vertebrae that articulate with chevron bones and those succeeding through the end of the column; the first is characterized by the anterior portion of the chevron articulating on the posterior side of the vertebra (Noble and Fraser 1971; Torre-Cosio 1995). A list of vertebral morphometrics is available in Table S1.

In SDNHM 20688, all vertebral epiphyses are fully fused to centra (vertebral bodies), suggesting the skeleton was physically mature. The first three cervical vertebrae are fused into a single block, and the last four are free. Complete vertebrarterial canals are present on both sides of the fifth vertebra. The neural arch is complete in all but the fourth cervical. The thoracic vertebrae increase in size to the last one. All the neural spines point upward with a slight concave shape. The lumbar vertebrae increase in size until the thirteenth. Their neural spines also point upward,

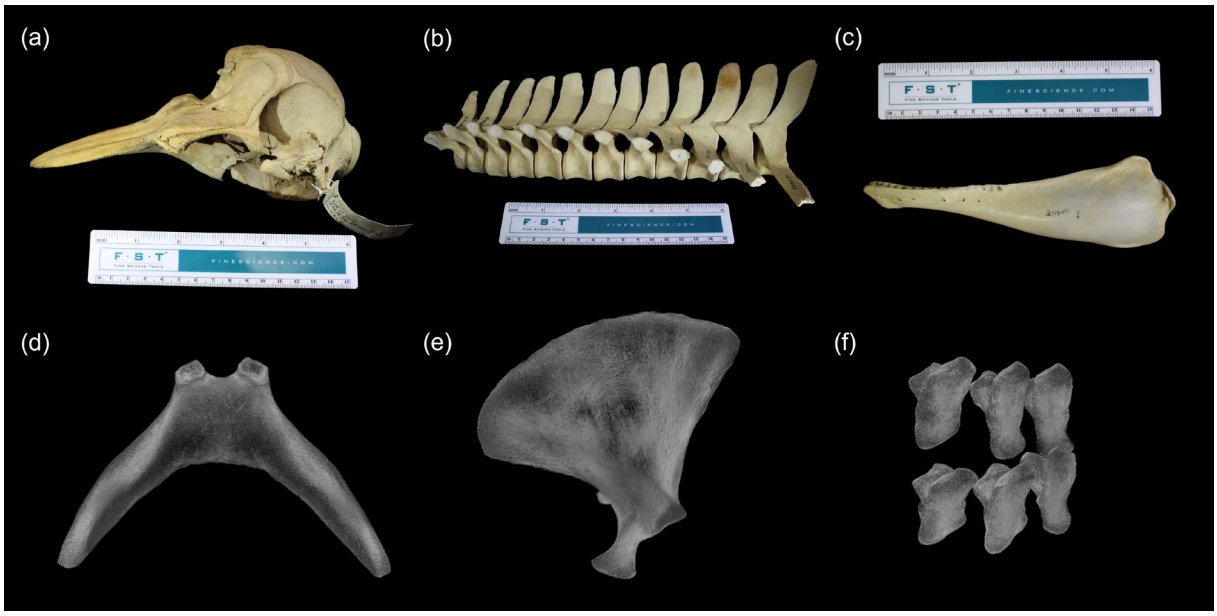

FIGURE 2 | Selected examples of SDNHM 20688 (*Phocoena sinus*) scientific photographs (a–c) and micro-CT volume renderings (d–f). (a) Skull, left lateral view, (b) Thoracic vertebrae #1–12, left lateral view, (c) Left mandible, exterior view, (d) Fused basihyal and thryohyals, ventral view, (e) Scapula, right, medial view, (f) Selected chevrons, three-quarter view. Photographs of all the bones can be found on MorphoSource.

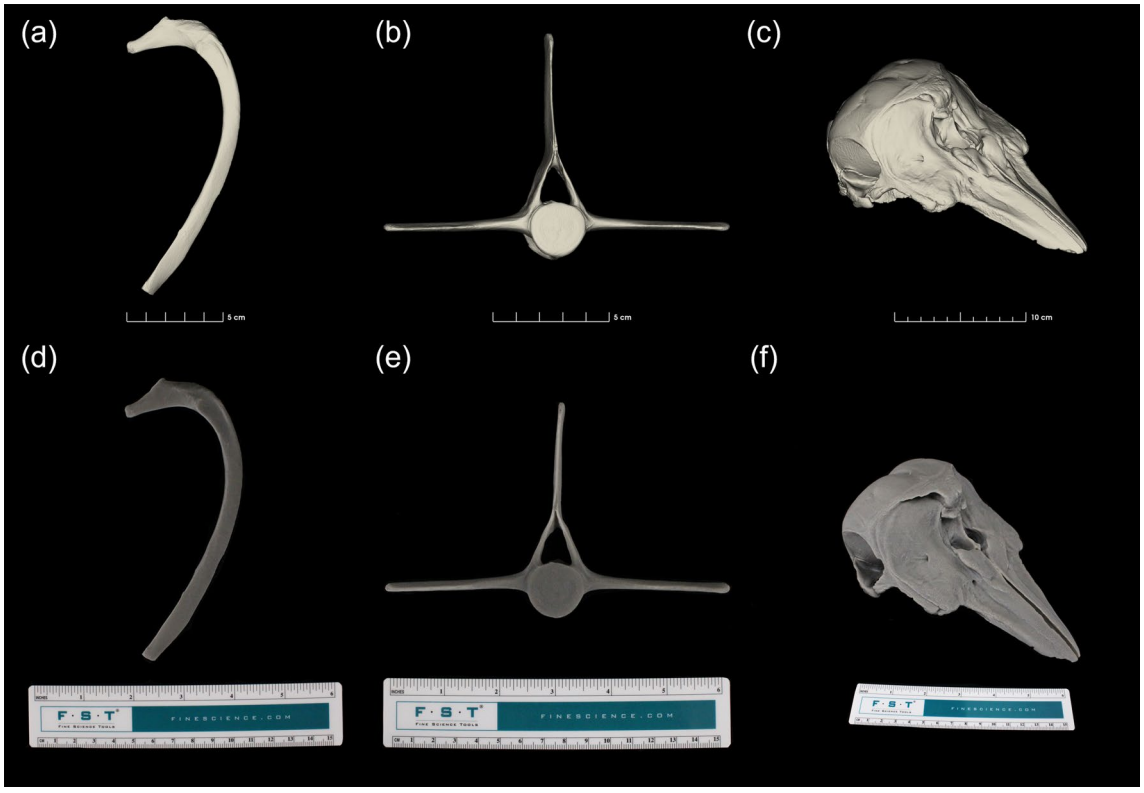

FIGURE 3 | Selected examples of SDNHM 20688 (*Phocoena sinus*) meshes (a–c) and photographs of associated 3D prints (d–f). (a, d) Right true rib, #2, (b, e) Lumbar vertebra #3, (c, f) Skull.

but starting with the second lumbar, the anterior edge becomes concave in lateral view. The left transverse processes of the sixth through eighth lumbar vertebrae exhibit remodeling approximately halfway down the process, which is consistent with healed fractures. Similar pathologies have been documented in the ribs and vertebrae of other vaquita specimens (see figure 7 of Noble and Fraser for vertebral fractures) and have been thought to originate from unsuccessful predation attempts, aggressive interactions with conspecifics, or interactions with common bottlenose dolphins (*Tursiops truncatus*), as reported with *P. phocoena* (Cotter et al. 2012; Gross et al. 2020; Noble and Fraser 1971; Ross and Wilson 1996; Torre-Cosio 1995; Vidal

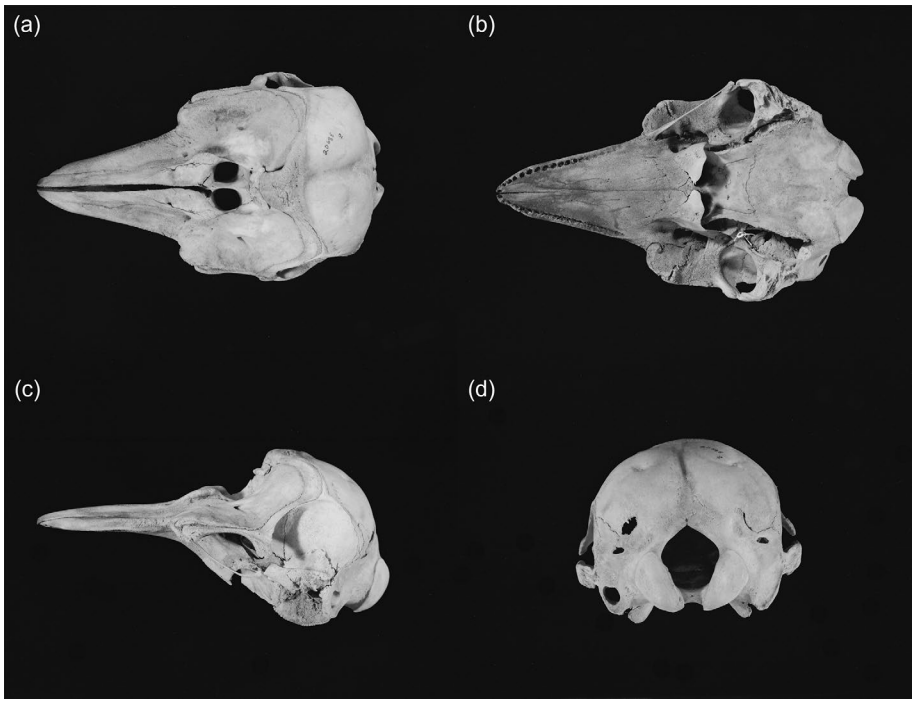

FIGURE 4 | Scanned negatives of the original film photography of SDNHM 20688 (*Phocoena sinus*) skull captured by Dallas Clites in 1968. (a) Dorsal view, (b) Ventral view, (c) Lateral view, and (d) Posterior view.

et al. 2024). The caudal vertebrae, starting with the second one, decrease in size posteriorly. The neural arches decrease in size posteriorly until the sixteenth vertebra, where they are absent. The transverse processes gradually decrease until the eleventh vertebra, where they are absent. Nineteen chevron bones (also referred to as hemal bones or hemapophyses) are present. The two halves of the first two chevrons and the last chevron are separated ventrally. The height increases from the third to the fourth chevron and stays consistent until decreasing after the seventh chevron. In the whole intact specimen, the anal opening was located below the junction of the fifth and sixth caudal vertebrae. The pelvic bones are vestigial (total length: 73 mm—left; 68 mm—right). As in all other small cetaceans, these bones are sexually dimorphic and smaller in females than in adult males (Dines et al. 2014; Goodall et al. 1988; Torre-Cosio 1995; Yoshida et al. 1994).

There are twelve pairs of true ribs, the first six being double-headed on both sides with capitular and tubercular attachments. A small floating thirteenth rib is present on the left side. The first rib, as in other cetaceans, is the stoutest, and the others become more slender posteriorly. Measurements of the true ribs are available in Table S2. There are seven sternal ribs on the left side, six on the right. The sternum is completely fused, representing the fusion of three separate bones. The first three anterior pairs of sternal ribs attach to the sternum laterally. In the flesh, the other sternal ribs were connected to a piece of cartilaginous tissue at the posterior end of the sternum.

The forelimb starts with the scapula, which is wider than high. The length of the acromion process is twice its width. The height and width of the coracoid process are about equal, except that the distal end is fan shaped. The right forelimb bones including the humerus, radius, ulna, carpals (radiale, intermedium, and ulnare), metacarpals, and phalanges were preserved in an articulated state by dried soft tissue. Portions of the left forelimb also remain articulated from desiccated tissue and include the humerus, radius, and ulna as one unit, and some distal phalanges (Figure 1). The humerus is thick with a spheroidal head. It is as long as the ulna, but smaller than the radius. The middle of the ulna is only half the diameter of the radius. The olecranal process on the ulna is well developed. The characters of the forelimbs in SDNHM 20688 are consistent with the size and shape reported in other *P. sinus* specimens (Torre-Cosio 1995).

The phalanx formula (excluding metacarpals) for this specimen was originally determined from radiographs of the forelimbs as: I-1, II-9, III-8, IV-4, V-0 (left), and I-1, II-8, III-8, IV-3, V-1 (right). However, high-resolution micro-CT scans resolved tiny terminal phalanges within the dried soft tissue distal of the fifth metacarpal in both the left and right forelimbs. While terminal phalanges of other digits have been lost between the time of the original radiographs and the micro-CT scans, by using both modalities we update the phalanx formula for this specimen to I-1, II-9, III-8, IV-4, V-2 (left), and I-1, II-8, III-8, IV-3, V-2 (right). This updated formula is consistent with ranges reported for other vaquita specimens (Fitzgerald 1970; Mellor et al. 2009; Torre-Cosio 1995).

Also, of note is the presence of a process in the distocaudal aspect of the third metacarpal in both the left and right forelimbs (Figure 5). This bilateral polydactyly is a character unique to the vaquita and has been observed consistently in other specimens (Cooper and Dawson 2009; Ortega Ortiz 1993; Ortega Ortiz et al. 2000; Torre-Cosio 1995; Villa-Ramírez et al. 1996). The number of phalanges in the supernumerary digit is known to vary, and in SDNHM 20688, it consists of one phalanx in both the left and right forelimbs (Ortega Ortiz et al. 2000). As in other adult vaquita

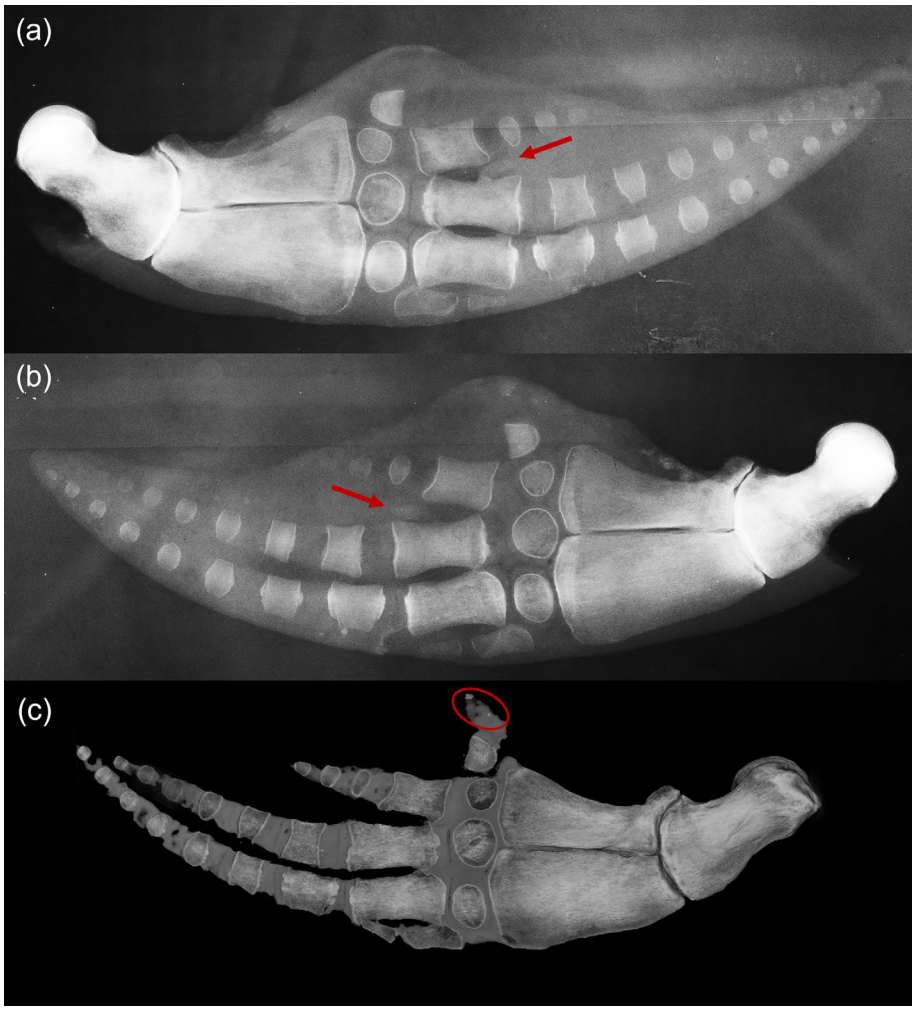

FIGURE 5 | SDNHM 20688 (*Phocoena sinus*) forelimbs. Radiographs of the (a) left and (b) right forelimb from the Providence Little Company of Mary Medical Center in Torrance, California, captured May 3, 1966. The supernumerary digit (polydactyly) is indicated by a red arrow. The micro-CT scan (c) of the right forelimb depicts the two phalanges of digit five (red circle) when only one was documented from the original radiographs.

specimens, the process is elongated and appears rhomboidal or trapezoidal in shape (Villa-Ramírez et al. 1996). While this extra process is apparent in the radiographs of the forelimb of SDNHM 20688, it was detached from metacarpal three at some point prior to micro-CT scanning and is not captured in the 3D data.

All data produced (photographs, micro-CT image stacks, and mesh files) are freely available for viewing and download from MorphoSource (Figure 6). This work, termed "The Vaquita Digitization Project," will allow scientists, researchers, teachers, students, and the public to view, download, and utilize these data. Below, we describe some ways that each type of data could be utilized for research, education, and other creative projects.

Derived media (photographs, medical CT scans, micro-CT scans, and 3D meshes) are available to view through MorphoSource or can be downloaded for use. All recent photographs include a scale bar, allowing for easy measuring through free software like ImageJ (Schneider et al. 2012). Additionally, photographs are available for use in educational displays, outreach events, or scientific study. The micro-CT scans can be downloaded and examined via free software (e.g., 3D Slicer) or explored through MorphoSource's 3D web viewer. This embedded feature allows viewers to explore the 2D slices of a scan and generate a 3D volume rendering. While our dataset consists of skeletal elements only, high-resolution micro-CT scans of porpoise anatomy (skeletal and soft-tissue) allow for use in a wide variety of research disciplines, including but not limited to vertebrate biology, ecology, functional morphology, comparative anatomy, evolutionary biology, pathology, diagnostics, and paleontology (Arribart et al. 2018; Baier-Stegmaier et al. 2023; Coombs et al. 2022; Dennison et al. 2012; Graïc et al. 2025; Huggenberger et al. 2008, 2009; Hunt et al. 2019; Kodera et al. 2022; Kot et al. 2018, 2019, 2022, 2024; Kuijpers et al. 2022; Kuroda et al. 2018; Lee et al. 2023, 2024; Marino et al. 2003; Moore et al. 2011; Murakami et al. 2012; Orbach et al. 2017; Racicot et al. 2014, 2016; Racicot and Berta 2013; Racicot and Colbert 2013; Racicot and Rowe 2014; Rolvien et al. 2017; Song et al. 2016, 2018, 2023; Wei et al. 2015, 2020; Willems et al. 2021; Yuen et al. 2017, 2022, 2024, 2025; Zhang et al. 2021). The meshes serve as realistic models and offer quick viewing in 3D rather than scrolling through 2D slices or requiring the user to generate a volume rendering. Additionally, the meshes were designed to support 3D printing for generating replicas that can be used in a variety of educational programs, as they are sturdy, easy to transport, and safe for hands-on activities for children, students, and the public. Physical engagement with 3D-printed bones offers a powerful connection between people

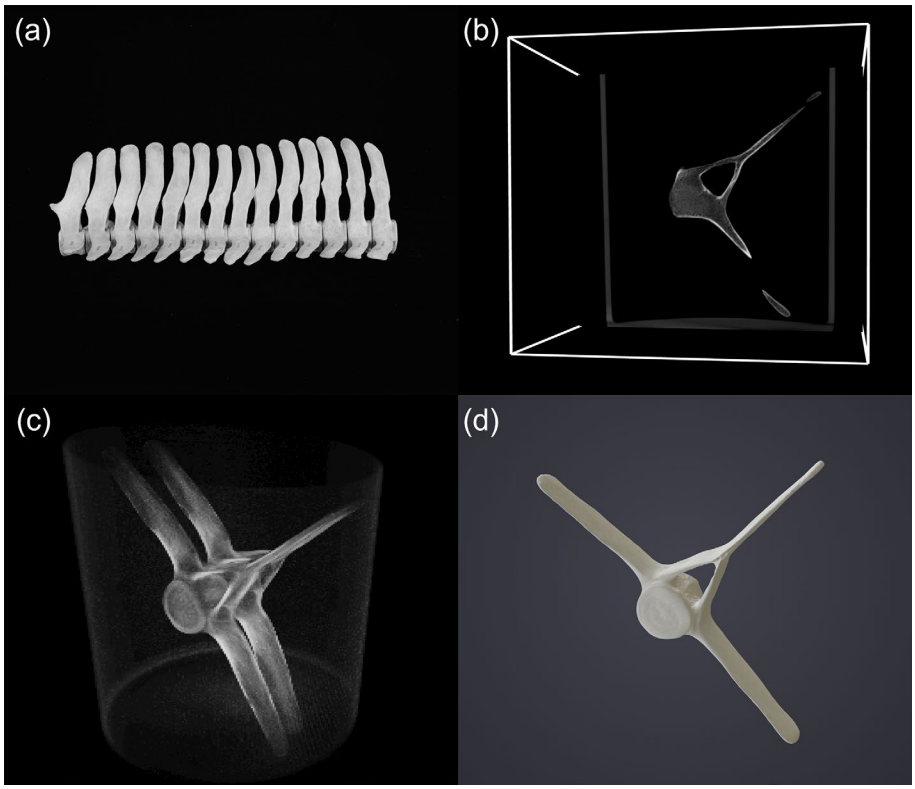

FIGURE 6 | Media viewing of the SDNHM 20688 (*Phocoena sinus*) dataset in MorphoSource. The main viewing page for each piece of media displays general details, file information, acquisition settings, and ownership permissions (not pictured). The main page also features an integrated viewing display for (a) photographs, (b, c) volumetric datasets, and (d) meshes. Vaquita media featured includes (a) a lateral view photograph of lumbar vertebrae #1–14, a micro-CT scan (b) slice view and (c) volume view of lumbar vertebrae #3–4, and (d) a mesh of lumbar vertebra #3.

and the vaquita, could help raise awareness, and allow for public display of this incredibly rare specimen.

The vaquita was first described in 1958 from three skulls found on the beach along the northwestern Gulf of California (Norris and McFarland 1958). Nearly 70 years later, the number of vaquita specimens in Mexican and U.S. collections outnumbers the remaining wild population by 12:1 (see list of museum specimens in Table S3). Given the vaquita's status as critically endangered and the significance of each specimen, all efforts should be made to preserve the vaquita digitally. This dataset serves as an accessible, permanent digital record of one of the rarest mammals on Earth, safeguarding invaluable morphological data for future research and education. By making this dataset openly available, we aim to support ongoing marine mammal science while also promoting awareness of biodiversity loss and inspiring further conservation efforts for the vaquita and other species facing extinction as the result of human impact.

Author Contributions

J.L.K. conceptualization, data curation, funding acquisition, investigation, methodology, project administration, visualization, writing – original draft. B.A.D. conceptualization, funding acquisition, investigation, project administration, resources, writing – review and editing. P.U. resources, writing – review and editing. R.L.B. resources, writing – original draft. T.L.M. conceptualization, funding acquisition, project administration, resources, supervision, writing – review and editing. M.E.P. conceptualization, funding acquisition, project administration, resources, supervision, writing – review and editing.

Acknowledgments

As this specimen predates the Marine Mammal Protection Act of 1972 and the vaquita's designation under the Endangered Species Act in 1985, specimen-specific permitting was not required for the loan between either SDNHM and SWC or SWC and FAU, per email communications between SWC and NMFS, Office of Protected Resources. The authors thank the late Raymond M. Gilmore, who aided R.L.B. in the dissection of the specimen in San Diego, and the late Richard C. Banks, who facilitated the deposit of the specimen into the SDNHM collection. The authors thank Gary Knaub for skillful scanning of the original film negatives developed by Dallas Cites, and the San Diego Zoo Wildlife Alliance for contributing the medical CT scans. The authors thank the handling editor Lisa N. Cooper and the two reviewers for the valuable comments. This work was produced in part using the Waygate Technologies Phoenix v|tome|x m 240 system at the Nanoscale Research Facility (RRID:SCR_025135) of the Herbert Wertheim College of Engineering at the University of Florida with the valuable assistance of Gary Scheiffele and financial support from SeaWorld California. This work was produced in part using the Bruker SkyScan 1173 micro-CT system in the Berlin Family Bioimaging Lab at the FAU Lab Schools Marcus Research and Innovation Center (RRID:SCR_023805). Open access to the dataset on MorphoSource was supported by FAU's School of Environmental, Coastal, and Ocean Sustainability (ECOS).

Funding

This work was supported by Florida Atlantic University School of Environmental, Coastal, and Ocean Sustainability (ECOS). Florida Atlantic University Laboratory Schools. SeaWorld California.

Conflicts of Interest

The authors declare no conflicts of interest.

Data Availability Statement

The data that support the findings of this study are openly available in MorphoSource at https://www.morphosource.org/projects/000681222?locale=en.

References

Aceves-Bueno, E., L. Davids, J. A. Rodriguez-Valencia, et al. 2023. "Derelict Gear From an Illegal Fishery: Lessons From Gear Retrieval Efforts in the Upper Gulf of California." *Marine Policy* 147: 105387. https://doi.org/10.1016/j.marpol.2022.105387.

Arribart, M., J. Ognard, C. Tavernier, et al. 2018. "Comparative Anatomical Study of Sound Production and Reception Systems in the Common Dolphin (*Delphinus delphis*) and the Harbour Porpoise (*Phocoena phocoena*) Heads." *Anatomia, Histologia, Embryologia* 47, no. 1: 3–10. https://doi.org/10.1111/ahe.12305.

Baier-Stegmaier, S., C. Gundlach, M. Chriél, et al. 2023. "Computed Tomography as a Method for Age Determination of Carnivora and Odontocetes With Validation From Individuals With Known Age." *Animals* 13, no. 11: 1783. https://doi.org/10.3390/ani13111783.

Ben-Hasan, A., Y. Sadovy de Mitcheson, M. A. Cisneros-Mata, et al. 2021. "China's Fish Maw Demand and Its Implications for Fisheries in Source Countries." *Marine Policy* 132: 104696. https://doi.org/10.1016/j.marpol.2021.104696.

Blackburn, D. C., D. M. Boyer, J. A. Gray, et al. 2024. "Increasing the Impact of Vertebrate Scientific Collections Through 3D Imaging: The openVertebrate (oVert) Thematic Collections Network." *Bioscience* 74, no. 3: 169–186. https://doi.org/10.1093/biosci/biad120.

Boyer, D. M., G. F. Gunnell, S. Kaufman, and T. M. McGeary. 2016. "Morphosource: Archiving and Sharing 3-D Digital Specimen Data." *Paleontological Society Papers* 22: 157–181. https://doi.org/10.1017/scs.2017.13.

Brownell, R. L. 1982. "Status of the Cochito, *Phocoena sinus*, in the Gulf of California".

Brownell, R. L. 1983. "*Phocoena sinus*." *Mammalian Species* 198: 1–3.

Brownell, R. L. 1986. "Distribution of the Vaquita, *Phocoena sinus*, in Mexican Waters." *Marine Mammal Science* 2, no. 4: 299–305.

Brownell, R. L., L. T. Findley, O. Vidal, A. Robles, and N. Silvia Manzanilla. 1987. "External Morphology and Pigmentation of the Vaquita, *Phocoena sinus* (Cetacea: Mammalia)." *Marine Mammal Science* 3, no. 1: 22–30. https://doi.org/10.1111/j.1748-7692.1987.tb00149.x.

Burmeister, H. 1865. "Description of a New Species of Porpoise in the Museum of Buenos Ayres." *Proceedings of the Zoological Society of London* 33, no. 1: 228–231. https://doi.org/10.1111/j.1469-7998.1865.tb02325.x.

Cardenas-Hinojosa, G., A. Jaramillo-Legorreta, A. Bonilla-Garzón, et al. 2024. "Survey Report for Vaquita Research 2024." https://iucn-csg.org/wp-content/uploads/2024/12/Reporte-Crucero-Vaquita-2024-Ingles-Final.pdf.

Cárdenas-Hinojosa, G., L. Rojas-Bracho, E. Nieto, et al. 2025. "Vaquita Research Campaign 2025: Report of the September Vaquita Survey." https://iucn-csg.org/wp-content/uploads/2025/11/Report-vaquita-acoustic-and-visual-survey-2025-EN-Nov-11-clean-FINAL.pdf.

Cisneros-Mata, M. A. 2020. *Evaluación de la Poblavión de Totoaba Macdonaldi*. INAPESCA.

Cisneros-Mata, M. A., G. Montemayor-López, and M. J. Román-Rodríguez. 1995. "Life History and Conservation of *Totoaba macdonaldi*." *Conservation Biology* 9, no. 4: 806–814.

Coombs, E. J., R. N. Felice, J. Clavel, et al. 2022. "The Tempo of Cetacean Cranial Evolution." *Current Biology* 32: 2233–2247.e4. https://doi.org/10.1016/j.cub.2022.04.060.

Cooper, L. N., A. Berta, S. D. Dawson, and J. S. Reidenberg. 2007. "Evolution of Hyperphalangy and Digit Reduction in the Cetacean Manus." *Anatomical Record* 290, no. 6: 654–672. https://doi.org/10.1002/ar.20532.

Cooper, L. N., and S. D. Dawson. 2009. "The Trouble With Flippers: A Report on the Prevalence of Digital Anomalies in Cetacea." *Zoological Journal of the Linnean Society* 155, no. 3: 722–735. https://doi.org/10.1111/j.1096-3642.2008.00454.x.

Cotter, M. P., D. Maldini, and T. A. Jefferson. 2012. ""Porpicide" in California: Killing of Harbor Porpoises (*Phocoena phocoena*) by Coastal Bottlenose Dolphins (*Tursiops truncatus*)." *Marine Mammal Science* 28, no. 1: E1–E15. https://doi.org/10.1111/j.1748-7692.2011.00474.x.

Cozzi, B., S. Huggenberger, and H. A. Oelschläger. 2016. *Anatomy of Dolphins: Insights Into Body Structure and Function*. Academic Press.

D'Agrosa, C., C. E. Lennert-Cody, and O. Vidal. 2000. "Vaquita Bycatch in Mexico's Artisanal Gillnet Fisheries: Driving a Small Population to Extinction." *Conservation Biology* 14, no. 4: 1110–1119. https://doi.org/10.1046/j.1523-1739.2000.98191.x.

D'Agrosa, C., O. Vidal, and W. C. Graham. 1995. "Mortality of the Vaquita (*Phocoena sinus*) in Gillnet Fisheries During 1993-94." *Reports of the International Whaling Commission Special Issues* 16: 283–294.

Dennison, S., A. Fahlman, and M. Moore. 2012. "The Use of Diagnostic Imaging for Identifying Abnormal Gas Accumulations in Cetaceans and Pinnipeds." *Frontiers in Physiology* 3: 181. https://doi.org/10.3389/fphys.2012.00181.

Dines, J. P., E. Otárola-Castillo, P. Ralph, et al. 2014. "Sexual Selection Targets Cetacean Pelvic Bones." *Evolution* 68, no. 11: 3296–3306. https://doi.org/10.1111/evo.12516.

Fitzgerald, G. D. 1970. *Comparative Morphology of the Forelimb Skeleton in Some Odontoceti (Mammalia, Cetacea)*. California State College at Long Beach.

Gerrodette, T., L. A. Fleischer, H. Perez-Cortes, and B. Villa-Ramírez. 1995. "Distribution of the Vaquita, *Phocoena sinus*, Based on Sightings From Systematic Surveys." *Reports of the International Whaling Commission (Special Issue)* 16: 273–281.

Gerrodette, T., B. L. Taylor, R. Swift, S. Rankin, A. M. Jaramillo-Legorreta, and L. Rojas-Bracho. 2011. "A Combined Visual and Acoustic Estimate of 2008 Abundance, and Change in Abundance Since 1997, for the Vaquita, *Phocoena sinus*." *Marine Mammal Science* 27, no. 2: E79–E100. https://doi.org/10.1111/j.1748-7692.2010.00438.x.

Goodall, R. N. P., A. R. Galeazzi, S. Leatherwood, et al. 1988. "Studies of Commerson's Dolphins, *Cephalorhynchus commersonii*, off Tierra del Fuego, 1976–1984." *Report of the International Whaling Commission (Special Issue 9)* 9: 143–160.

Graïc, J.-M., T. Gerussi, B. Cozzi, et al. 2025. "A Contribution to the Anatomy of Two Rare Cetacean Species: The Hourglass Dolphin (*Cephalorhynchus cruciger*) and the Spectacled Porpoise (*Phocoena dioptrica*)." *Anatomical Record* n/a, no. n/a: ar.70045. https://doi.org/10.1002/ar.70045.

Gray, J. A., E. L. Stanley, C. M. Sheehy III, Z. S. Randall, G. J. Watkins-Colwell, and D. C. Blackburn. 2025. "The Diffusion Diaries: Diffusible Iodine-Based Contrast-Enhanced Computed Tomography for Vertebrate Natural History Specimens." *Integrative Organismal Biology* 7, no. 1: obaf014. https://doi.org/10.1093/iob/obaf014.

Gross, S., P. Claus, P. Wohlsein, et al. 2020. "Indication of Lethal Interactions Between a Solitary Bottlenose Dolphin (*Tursiops truncatus*) and Harbor Porpoises (*Phocoena phocoena*) in the German Baltic Sea." *BMC Zoology* 5, no. 1: 12. https://doi.org/10.1186/s40850-020-00061-7.

Howes, G. B. 1880. "Some Points in the Anatomy of the Porpoise (*Phocœna communis*)." *Journal of Anatomy and Physiology* 14, no. Pt 4: 467–474.

Huggenberger, S., M. A. Rauschmann, and H. H. A. Oelschläger. 2008. "Functional Morphology of the Hyolaryngeal Complex of the Harbor Porpoise (*Phocoena phocoena*): Implications for Its Role in Sound Production and Respiration." *Anatomical Record* 291: 1262–1270. https://doi.org/10.1002/ar.20745.

Huggenberger, S., M. A. Rauschmann, T. J. Vogl, and H. H. A. Oelschläger. 2009. "Functional Morphology of the Nasal Complex in the Harbor Porpoise (*Phocoena phocoena L.*)." *Anatomical Record* 292, no. 6: 902–920. https://doi.org/10.1002/ar.20854.

Hunt, R., S. Trabia, Z. Olsen, and K. Kim. 2019. "A Soft-Robotic Harbor Porpoise Pectoral Fin Driven by Coiled Polymer Actuators as Artificial Muscles." *Advanced Intelligent Systems* 1, no. 4: 1900028. https://doi.org/10.1002/aisy.201900028.

Jaramillo-Legorreta, A., A. Bonilla-Garzón, G. Cardenas-Hinojosa, et al. 2023. "Vaquita-Survey-2023-Main-Report." https://iucn-csg.org/wp-content/uploads/2023/06/Vaquita-Survey-2023-Main-Report.pdf.

Jaramillo-Legorreta, A., G. Cardenas-Hinojosa, E. Nieto-Garcia, et al. 2017. "Passive Acoustic Monitoring of the Decline of Mexico's Critically Endangered Vaquita." *Conservation Biology* 31, no. 1: 183–191. https://doi.org/10.1111/cobi.12789.

Jaramillo-Legorreta, A., G. Cardenas-Hinojosa, E. Nieto-Garcia, et al. 2019. "Decline Towards Extinction of Mexico's Vaquita Porpoise (*Phocoena sinus*)." *Royal Society Open Science* 6, no. 7: 190598. https://doi.org/10.1098/rsos.190598.

Jaramillo-Legorreta, A., L. Rojas-Bracho, and T. Gerrodette. 1999. "A New Abundance Estimate for Vaquitas: First Step for Recovery." *Marine Mammal Science* 15, no. 4: 957–973. https://doi.org/10.1111/j.1748-7692.1999.tb00872.x.

Jefferson, T. A., P. A. Olson, T. R. Kieckhefer, and L. Rojas-Bracho. 2009. "Photo-Identification of the Vaquita (*Phocoena sinus*): The World's Most Endangered Cetacean." *Latin American Journal of Aquatic Mammals* 7: 53–56. https://doi.org/10.5597/lajam00134.

Jefferson, T. A., M. A. Webber, and R. L. Pitman. 2015. "4—Cetaceans." In *Marine Mammals of the World*, Edited by T. A. Jefferson, M. A. Webber, and R. L. Pitman, Second ed., 24–357. Academic Press. https://doi.org/10.1016/B978-0-12-409542-7.50004-4.

Kasuya, T. 1973. "Systematic Consideration of Recent Toothed Whales Based on the Morphology of Tympano-Periotic Bone." *Scientific Reports of the Whales Research Institute* 25: 1–103.

Kodera, R., Y. Uekusa, K. Ito, N. Kuroda, H. Kodera, and H. Endo. 2022. "An Anatomical Study of the Subpulpal Wall of Abnormal Multirooted Teeth in the Narrow-Ridged Finless Porpoise (*Neophocaena asiaeorientalis*)." *Marine Mammal Science* 38, no. 2: 557–570. https://doi.org/10.1111/mms.12884.

Kot, B. C. W., D. K. P. Chan, A. H. L. Yuen, and H. C. L. Tsui. 2018. "Diagnosis of Atlanto-Occipital Dissociation: Standardised Measurements of Normal Craniocervical Relationship in Finless Porpoises (*Genus neophocaena*) Using Postmortem Computed Tomography." *Scientific Reports* 8, no. 1: 8474. https://doi.org/10.1038/s41598-018-26866-8.

Kot, B. C. W., D. K. P. Chan, A. H. L. Yuen, F. H. M. Wong, and H. C. L. Tsui. 2019. "Morphological Analysis of the Foramen Magnum in Finless Porpoise (*Genus neophocaena*) Using Postmortem Computed Tomography 3D Volume Rendered Images." *Marine Mammal Science* 35, no. 1: 261–270. https://doi.org/10.1111/mms.12512.

Kot, B. C. W., H. H. N. Ho, E. K. C. Leung, T. Y. T. Chung, and H. C. L. Tsui. 2022. "Characterisation of *Crassicauda fuelleborni* Nematode Infection in Indo-Pacific Finless Porpoises (*Neophocaena phocaenoides*) Using Postmortem Computed Tomography." *International Journal for Parasitology: Parasites and Wildlife* 18: 68–75. https://doi.org/10.1016/j.ijppaw.2022.04.005.

Kot, B. C. W., J. W. Y. Yeong, A. S. Y. Kwan, et al. 2024. "Illustrated Cross-Sectional Computed Tomography of the Cetacean Abdomino-Pelvic Organs." *Annals of Anatomy—Anatomischer Anzeiger* 256: 152317. https://doi.org/10.1016/j.aanat.2024.152317.

Kuijpers, N. W., L. van Schalkwijk, L. L. IJsseldijk, et al. 2022. "Post-Mortem Computed Tomography Pulmonary Findings in Harbor Porpoises (*Phocoena phocoena*)." *Animals* 12, no. 11: 1–14. https://doi.org/10.3390/ani12111454.

Kuroda, M., M. Sasaki, K. Yamada, N. Miki, N. Matsui, and T. Matsuishi. 2018. "Click Emission in Dall's Porpoise *Phocoenoides dalli*, Focusing on Physical Properties of Tissues." *PLoS One* 13, no. 9: e0202426. https://doi.org/10.1371/journal.pone.0202426.

Lagomarsino, I. V. 1991. "Endangered Species Status Review." In Totoaba Macdonaldi. National Marine Fisheries Service, Southwest Region.

Lahille, F. 1912. "Nota Preliminar Sobre Una Nueva Especie de Marsopa del río de la Plata, *Phocoena Dioptrica*." *Anales del Museo Nacional de Historia Natural de Buenos Aires* 23: 269–278.

Lee, S. B., A. H. L. Yuen, S. Kim, et al. 2024. "Ingestion of Fishing Gear and Anisakis sp. Infection in a Beached Indo-Pacific Finless Porpoise (*Neophocaena phocaenoides*) in the Jeju Island, Republic of Korea: Findings From Post-Mortem Computed Tomography and Necropsy." *BMC Veterinary Research* 20, no. 1: 232. https://doi.org/10.1186/s12917-024-04090-z.

Lee, S. B., A. H. L. Yuen, Y. M. Lee, et al. 2023. "Adhesive Bowel Obstruction (ABO) in a Stranded Narrow-Ridged Finless Porpoise (*Neophocaena asiaeorientalis sunameri*)." *Animals* 13, no. 24: 3767. https://doi.org/10.3390/ani13243767.

Magatagan, M. D., E. H. Boyer, and B. Villa-Ramírez. 1984. "Revisión del estado que guarda *Phocoena sinus* Norris and McFarland y descripción de tres nuevos ejemplares." *Anales del Instituto de Biología, UNAM, Serie Zoología* 55, no. 1: 271–293.

Marino, L., M. D. Uhen, N. D. Pyenson, and B. Frohlich. 2003. "Reconstructing Cetacean Brain Evolution Using Computed Tomography." *Anatomical Record Part B: The New Anatomist* 272B, no. 1: 107–117. https://doi.org/10.1002/ar.b.10018.

Mellor, L., L. Cooper, J. Torre, and R. L. Brownell. 2009. "Paedomorphic Ossification in Porpoises With an Emphasis on the Vaquita (*Phocoena sinus*)." *Aquatic Mammals* 35: 193–202. https://doi.org/10.1578/AM.35.2.2009.193.

Messenger, S. L., and J. A. McGuire. 1998. "Morphology, Molecules, and the Phylogenetics of Cetaceans." *Systematic Biology* 47, no. 1: 90–124. https://doi.org/10.1080/106351598261058.

Moore, M. J., T. Hammar, J. Arruda, et al. 2011. "Hyperbaric Computed Tomographic Measurement of Lung Compression in Seals and Dolphins." *Journal of Experimental Biology* 214, no. 14: 2390–2397. https://doi.org/10.1242/jeb.055020.

Morin, P. A., F. I. Archer, C. D. Avila, et al. 2021. "Reference Genome and Demographic History of the Most Endangered Marine Mammal, the Vaquita." *Molecular Ecology Resources* 21, no. 4: 1008–1020. https://doi.org/10.1111/1755-0998.13284.

Murakami, M., C. Shimada, Y. Hikida, and H. Hirano. 2012. "A New Basal Porpoise, *Pterophocaena nishinoi* (Cetacea, Odontoceti, Delphinoidea), from the Upper Miocene of Japan and Its Phylogenetic Relationships." *Journal of Vertebrate Paleontology* 32, no. 5: 1157–1171. https://doi.org/10.1080/02724634.2012.677299.

Noble, B. A., and F. C. Fraser. 1971. "Description of a Skeleton and Supplementary Notes on the Skull of a Rare Porpoise *Phocoena sinus* Norris & McFarland 1958." *Journal of Natural History* 5, no. 4: 447–464. https://doi.org/10.1080/00222937100770311.

Norris, K. S., and W. N. McFarland. 1958. "A New Harbor Porpoise of the Genus *Phocoena* From the Gulf of California." *Journal of Mammalogy* 39, no. 1: 22. https://doi.org/10.2307/1376606.

Orbach, D. N., D. A. Kelly, M. Solano, and P. L. R. Brennan. 2017. "Genital Interactions During Simulated Copulation Among Marine Mammals." *Proceedings of the Royal Society B: Biological Sciences* 284, no. 1864: 20171265. https://doi.org/10.1098/rspb.2017.1265.

Ortega Ortiz, J. G. 1993. "Descripción Osteológica de la Aleta Pectoral de la Vaquita Phocoena Sinus (Cetacea: Phocoenidae) [B.Sc. Thesis]. Universidad Nacional Autónoma de México".

Ortega Ortiz, J. G., B. Villa-Ramírez, and J. R. Gersenowies. 2000. "Polydactyly and Other Features of the Manus of the Vaquita, *Phocoena sinus*." *Marine Mammal Science* 16, no. 2: 277–286.

Perrin, W. F., R. N. P. Goodall, and M. A. Cozzuol. 2000. "Osteological Variation in the Spectacled Porpoise (*Phocoena dioptrica*)." *Journal of Cetacean Research and Management* 2, no. 3: 211–215. https://doi.org/10.47536/jcrm.v2i3.909.

Racicot, R. A., and A. Berta. 2013. "Comparative Morphology of Porpoise (Cetacea: Phocoenidae) Pterygoid Sinuses: Phylogenetic and Functional Implications." *Journal of Morphology* 274, no. 1: 49–62. https://doi.org/10.1002/jmor.20075.

Racicot, R. A., and M. W. Colbert. 2013. "Morphology and Variation in Porpoise (Cetacea: Phocoenidae) Cranial Endocasts." *Anatomical Record* 296, no. 6: 979–992. https://doi.org/10.1002/ar.22704.

Racicot, R. A., T. A. Deméré, B. L. Beatty, and R. W. Boessenecker. 2014. "Unique Feeding Morphology in a New Prognathous Extinct Porpoise From the Pliocene of California." *Current Biology* 24, no. 7: 774–779. https://doi.org/10.1016/j.cub.2014.02.031.

Racicot, R. A., W. Gearty, N. Kohno, and J. J. Flynn. 2016. "Comparative Anatomy of the Bony Labyrinth of Extant and Extinct Porpoises (Cetacea: Phocoenidae)." *Biological Journal of the Linnean Society* 119, no. 4: 831–846. https://doi.org/10.1111/bij.12857.

Racicot, R. A., and T. Rowe. 2014. "Endocranial Anatomy of a New Fossil Porpoise (Odontoceti, Phocoenidae) From the Pliocene San Diego Formation of California." *Journal of Paleontology* 88, no. 4: 652–663. https://doi.org/10.1666/13-109.

Reidenberg, J. S., and J. T. Laitman. 1994. "Anatomy of the Hyoid Apparatus in Odontoceti (Toothed Whales): Specializations of Their Skeleton and Musculature Compared With Those of Terrestrial Mammals." *Anatomical Record* 240, no. 4: 598–624. https://doi.org/10.1002/ar.1092400417.

Robinson, J. A., C. C. Kyriazis, S. F. Nigenda-Morales, et al. 2022. "The Critically Endangered Vaquita Is Not Doomed to Extinction by Inbreeding Depression." *Science* 376, no. 6593: 635–639. https://doi.org/10.1126/science.abm1742.

Rojas-Bracho, L., C. Booth, B. Taylor, L. Thomas, T. Gerrodette, and A. Henry. 2019a. "Report on Using Expert Elicitation to Estimate Total Unique Vaquitas and Calves in the Zero Tolerance Area With Recommendations for Future Research Efforts." https://iucn-csg.org/wp-content/uploads/2021/04/Vaquita-Report-on-Using-Expert-Elicitation-Final.pdf.

Rojas-Bracho, L., R. C. Brusca, S. Álvarez-Borrego, et al. 2019b. "Unsubstantiated Claims Can Lead to Tragic Conservation Outcomes." *Bioscience* 69, no. 1: 12–14. https://doi.org/10.1093/biosci/biy138.

Rojas-Bracho, L., F. M. D. Gulland, C. R. Smith, et al. 2019c. "A Field Effort to Capture Critically Endangered Vaquitas *Phocoena sinus* for Protection From Entanglement in Illegal Gillnets." *Endangered Species Research* 38: 11–27. https://doi.org/10.3354/esr00931.

Rojas-Bracho, L., B. Taylor, C. Booth, et al. 2022. "More Vaquita Porpoises Survive Than Expected." *Endangered Species Research* 48: 225–234. https://doi.org/10.3354/esr01197.

Rojas-Bracho, L., and B. L. Taylor. 1999. "Risk Factors Affecting the Vaquita (*Phocoena sinus*)." *Marine Mammal Science* 15, no. 4: 974–989. https://doi.org/10.1111/j.1748-7692.1999.tb00873.x.

Rolfe, S., S. Pieper, A. Porto, et al. 2021. "SlicerMorph: An Open and Extensible Platform to Retrieve, Visualize and Analyse 3D Morphology." *Methods in Ecology and Evolution* 12, no. 10: 1816–1825. https://doi.org/10.1111/2041-210X.13669.

Rolvien, T., M. Hahn, U. Siebert, et al. 2017. "Vertebral Bone Microarchitecture and Osteocyte Characteristics of Three Toothed Whale Species With Varying Diving Behaviour." *Scientific Reports* 7: 1604. https://doi.org/10.1038/s41598-017-01926-7.

Román-Rodríguez, M. J. 1990. "Alimentación de *Totoaba Macdonaldi* (Gilbert) (Pisces: Sciaenidae) en la Parte Norte del Alto Golfo de California." *Ecológica* 1, no. 2: 1–9.

Ross, H. M., and B. Wilson. 1996. "Violent Interactions Between Bottlenose Dolphins and Harbour Porpoises." *Proceedings of the Royal Society B: Biological Sciences* 263, no. 1368: 283–286. https://doi.org/10.1098/rspb.1996.0043.

Schneider, C. A., W. S. Rasband, and K. W. Eliceiri. 2012. "NIH Image to ImageJ: 25 Years of Image Analysis." *Nature Methods* 9, no. 7: 671–675. https://doi.org/10.1038/nmeth.2089.

Slijper, E. J. 1936. "Die Cetaceen. Vergleichend-anatomisch und systematisch." *Capita Zoologica* 590.

Smith, G. J. D., K. W. Browne, and D. E. Gaskin. 1976. "Functional Myology of the Harbour Porpoise, *Phocoena phocoena* (L.)." *Canadian Journal of Zoology* 54, no. 5: 716–729. https://doi.org/10.1139/z76-083.

Song, Z., W. Ou, J. Li, et al. 2023. "Sound Reception in the Yangtze Finless Porpoise and Its Extension to a Biomimetic Receptor." *Biomimetics* 8, no. 4: 366. https://doi.org/10.3390/biomimetics8040366.

Song, Z., Y. Zhang, T. A. Mooney, X. Wang, A. B. Smith, and X. Xu. 2018. "Investigation on Acoustic Reception Pathways in Finless Porpoise (*Neophocaena Asiaorientalis Sunameri*) With Insight Into an Alternative Pathway." *Bioinspiration & Biomimetics* 14, no. 1: 016004. https://doi.org/10.1088/1748-3190/aaeb01.

Song, Z., Y. Zhang, X. Wang, C. Wei, and P. Berggren. 2016. "Comparison of Acoustic Structures Between Heads of a Narrow-Ridged Finless Porpoise Fetus and Its Mother." *Journal of Mammalogy* 97, no. 4: 1074–1080. https://doi.org/10.1093/jmammal/gyw057.

Taylor, B. L., and T. Gerrodette. 1993. "The Uses of Statistical Power in Conservation Biology: The Vaquita and Northern Spotted Owl." *Conservation Biology* 7, no. 3: 489–500.

Taylor, B. L., L. Rojas-Bracho, J. Moore, et al. 2017. "Extinction Is Imminent for Mexico's Endemic Porpoise Unless Fishery Bycatch Is Eliminated." *Conservation Letters* 10, no. 5: 588–595. https://doi.org/10.1111/conl.12331.

Taylor, B. L., R. S. Wells, P. A. Olson, et al. 2019. "Likely Annual Calving in the Vaquita, *Phocoena sinus*: A New Hope?" *Marine Mammal Science* 35, no. 4: 1603–1612. https://doi.org/10.1111/mms.12595.

Thomas, L., A. Jaramillo-Legorreta, G. Cardenas-Hinojosa, et al. 2017. "Last Call: Passive Acoustic Monitoring Shows Continued Rapid Decline of Critically Endangered Vaquita." *Journal of the Acoustical Society of America* 142, no. 5: EL512. https://doi.org/10.1121/1.5011673.

Torre-Cosio, J. 1995. "Descripción Del Esqueleto, Dimorfismo Sexual y Crecimiento Alometrico en el Craneo de la Vaquita [M.Sc. Thesis]. Instituto Tecnológico y de Estudios Superiores de Monterrey Campus Guaymas".

Tyson, E. 1680. *Phocoena, or the Anatomy of a Porpess, Dissected at Gresham College*. B. Tooke.

Valenzuela-Quiñonez, F., F. Arreguín-Sánchez, S. Salas-Márquez, et al. 2015. "Critically Endangered Totoaba *Totoaba macdonaldi*: Signs of Recovery and Potential Threats After a Population Collapse." *Endangered Species Research* 29: 1–11. https://doi.org/10.3354/esr00693.

Vidal, O. 1995. "Population Biology and Incidental Mortality of the Vaquita, *Phocoena sinus*." *Reports of the International Whaling Commission, Special Issue* 16: 247–272.

Vidal, O., R. L. Brownell Jr, L. T. Findley, J. Torre, and R. C. Brusca. 2024. "Vaquita *Phocoena sinus* Norris and McFarland, 1958." In *Ridgway and Harrison's Handbook of Marine Mammals: Coastal Dolphins and Porpoises*, Edited by T. A. Jefferson, vol. 1, 487–518. Academic Press. https://doi.org/10.1016/B978-0-443-13746-4.00015-9.

Villa-Ramírez, B., M. Peralta-Perez, and A. Delgada-Estrella. 1996. "Description of the Third Metacarpal Axial Process in the Pectoral Fins of *Phocoena sinus*." *Contributions in Mammalogy: A Memorial Volume Honoring Dr. J. Knox Jones, Jr*: 205–208. https://www.si.edu/object/siris_sil_512053.

Wei, C., W. W. L. Au, and D. R. Ketten. 2020. "Modeling of the Near to Far Acoustic Fields of an Echolocating Bottlenose Dolphin and Harbor Porpoise." *Journal of the Acoustical Society of America* 147, no. 3: 1790–1801. https://doi.org/10.1121/10.0000918.

Wei, C., Z. Wang, Z. Song, et al. 2015. "Acoustic Property Reconstruction of a Neonate Yangtze Finless Porpoise's (*Neophocaena asiaeorientalis*) Head Based on CT Imaging." *PLoS One* 10, no. 4: e0121442. https://doi.org/10.1371/journal.pone.0121442.

Weisbecker, V., D. Fusco, S. Ingleby, et al. 2025. "Ozboneviz: An Australian Precedent in FAIR 3D Imagery and Extended Biodiversity Collections." *Bioscience* 75, no. 9: 747–756. https://doi.org/10.1093/biosci/biaf064.

Willems, D. S., L. L. IJsseldijk, D. H. N. van den Broek, and S. Veraa. 2021. "Vertebral Pattern Variation in the North Sea Harbor Porpoise (*Phocoena phocoena*) by Computed Tomography." *Anatomical Record* 304, no. 5: 968–978. https://doi.org/10.1002/ar.24524.

Yoshida, H., M. Shirakihara, A. Takemura, and K. Shirakihara. 1994. "Development, Sexual Dimorphism, and Individual Variation in the Skeleton of the Finless Porpoise, *Neophocaena phocaenoides*, in the Coastal Waters of Western Kyushu, Japan." *Marine Mammal Science* 10, no. 3: 266–282. https://doi.org/10.1111/j.1748-7692.1994.tb00482.x.

Yuen, A. H. L., S. W. Kim, S. B. Lee, et al. 2022. "Radiological Investigation of Gas Embolism in the East Asian Finless Porpoise (*Neophocaena asiaeorientalis sunameri*)." *Frontiers in Marine Science* 9: 1–10. https://doi.org/10.3389/fmars.2022.711174.

Yuen, A. H. L., S. B. Lee, S. W. Kim, et al. 2024. "Fatal Upper Aerodigestive Tract Obstruction in an East Asian Finless Porpoise (*Neophocaena asiaeorientalis sunameri*): Findings in Post-Mortem Computed Tomography." *Forensic Science, Medicine and Pathology* 20, no. 2: 644–651. https://doi.org/10.1007/s12024-023-00732-0.

Yuen, A. H. L., J.-H. Park, K. C. W. Chan, et al. 2025. "Optimizing diceCT Protocols for Post-Mortem Cetacean Imaging: Diffusible Iodine Enhancement of a Rare Narrow-Ridged Finless Porpoise (*Neophocaena asiaeorientalis*) Fetal Specimen Using Clinical-Grade Computed Tomography." *BMC Veterinary Research* 22: 29. https://doi.org/10.1186/s12917-025-05191-z.

Yuen, A. H. L., H. C. L. Tsui, and B. C. W. Kot. 2017. "Accuracy and Reliability of Cetacean Cranial Measurements Using Computed Tomography Three Dimensional Volume Rendered Images." *PLoS One* 12, no. 3: e0174215. https://doi.org/10.1371/journal.pone.0174215.

Zhang, Z.-X., J. Gong, S.-B. Yu, et al. 2021. "A Specialized Myodural Bridge Named Occipital-Dural Muscle in the Narrow-Ridged Finless Porpoise (*Neophocaena asiaeorientalis*)." *Scientific Reports* 11, no. 1: 15485. https://doi.org/10.1038/s41598-021-95070-y.

Supporting Information

Additional supporting information can be found online in the Supporting Information section. **Table S1:** Vertebral morphometrics of SDNHM 20688. Measurements were collected as follows: height—distance from ventral-most portion of the centrum to the tip of the neural process, width –distance from tips of transverse processes, length—distance from cranial to caudal face of vertebral centra. **Table S2:** Overall true rib lengths for SDNHM 20688. Length was measured as greatest distance between the highest point (head, neck, or angle) to tip of the costal end. **Table S3:** Vaquita (*Phocoena sinus*) specimens in U.S., UK, and Mexican collections. Catalog numbers are provided for all specimens which can be searched in several online biodiversity collection databases (GBIF, iDigBio, VertNet, etc.,) for additional information. Facility abbreviations (CAS = California Academy of Sciences, CEDO = Center for the Study of Desert and Oceans, CIAD = Centro de Investigación en Alimentación y Desarrollo, A.C., FCMM = Facultad de Ciencias, Universidad Nacional Autónoma de México, IBUNAM = Instituto de Biología, Universidad Nacional Autónoma de México, ITESM = Instituto Tecnológico y de Estudios Superiores de Monterrey, LACM = Natural History Museum of Los Angeles County, MBCM = Museo de La Ballena y Ciencias del Mar, MCZ = Museum of Comparative Zoology, MHN = Museo de Historia Natural de la Universidad Autónoma de Baja California Sur, MVZ = Museum of Vertebrate Zoology, NHMUK = Natural History Museum London, SDNHM = San Diego Natural History Museum, SWFC = Southwest Fisheries Science Center, UALP = University of Arizona Laboratory of Paleontology, USNM = Smithsonian National Museum of Natural History). **Video S1:** Reconstructed micro-CT scan of SDNHM 20688 right forelimb. Dried soft tissue has preserved the bones in an articulated state.